

# Improving the Performance of Motor Drive Servo Systems via Composite Nonlinear Control

Guoyang Cheng, *Senior Member, IEEE*, Wentao Yu, and Jin-gao Hu

**Abstract**—This paper presents a discrete-time design of robust composite nonlinear controller to achieve fast and accurate set-point tracking for motor servo systems subject to actuator saturation and disturbances. The basic idea here is to use a combination of linear and nonlinear control, together with a disturbance rejection mechanism based on extended state observer. The linear control part is designed to yield a fast response, and the nonlinear part serves to reduce the overshoot, while the extended state observer estimates simultaneously the state vector and the unknown disturbance for control and compensation. The closed-loop stability is analyzed using the Lyapunov theory. Practical application in a permanent magnet synchronous motor position servo system is given to demonstrate the effectiveness of the proposed control scheme.

**Index Terms**—Disturbance rejection, motion control, nonlinear control, observer, servo systems, transient performance.

## I. INTRODUCTION

SERVO control is essential for many industrial production and assembly lines, as well as for daily facilities, such as elevators. The main objective in servo system design is to ensure fast targeting and accurate tracking in the face of power limitation, various disturbances and uncertainties in real application environment. So far, this topic has been extensively studied and many control schemes have been developed, ranging from conventional proportional-integral derivative (PID) control to more advanced control techniques. Due to its simple structure, robustness and independence of plant model, PID is the dominant control technique used in industrial control [1]. However, the performance of PID control system might be far from desirable, if its parameters are not carefully tuned [2]. PID is of one degree-of-freedom structure and has the inherent limitation of linear control, i.e., a fast response and a low overshoot cannot be achieved at the same time with a given bandwidth. More over, PID is prone to the headache of integrator windup, when the plant is subjected to a large variation of set-point and/or disturbance. To improve the performance of PID control systems, a variety of modifications

have been proposed, e.g., nonlinear PID [3], [4], anti-windup PID [5], [6], variable gain PID [7-9]. These modified PID control techniques may bring along better performance, but will lead to a more complicated controller. Some of the modifications are based on the knowledge of model parameters, which is a self-defeat for what PID controllers usually boast about. To design a better controller with a simple structure for general plants, Han proposed the active disturbance rejection control (ADRC) scheme in [10], [11], which consists of a tracking differentiator for extracting the smooth derivatives from the target reference, a nonlinear extended state observer (ESO) to reconstruct the state variables and unknown lumped disturbance, and a nonlinear feedback control law based on state error. The ADRC scheme has attracted a lot of attention from the academic circle, and many research efforts and applications related to ADRC have been reported, see e.g., [12-16]. However, due to the difficulties in parameter tuning and stability analysis of the nonlinear dynamics in ADRC, research interests are shifting towards the linear ADRC control scheme, see e.g., [17-20].

In this paper, a framework of combined linear and nonlinear control will be adopted, so as to improve the transient performance of motor drive servo systems. The idea here can be traced back to the paper by Lin et al. [21], which introduced an additional nonlinear feedback term to speed up the settling process of set-point tracking tasks on second-order linear systems with input saturation. The idea was then extended to more general linear systems with measurement feedback by Chen et al. [22], and the name of composite nonlinear feedback (CNF) control was formerly used. The linear control part of CNF is designed such that the closed-loop system has a pair of lightly-damped dominant poles so as to gain a fast output response, while the nonlinear control part is used to tune up the closed-loop damping ratio for reducing the overshoot when the system output approaches the target reference. The CNF control technique is very attractive for its superior transient performance in set-point tracking, and no explicit switching element is involved in the controller. So far, successful applications of CNF control have been reported, e.g., hard disk drive servo system [22], [23], [24], flight control system for unmanned helicopters [25], [26], and grid-connected voltage source inverter [27].

The CNF control technique, as presented in [21], [22], assumes no disturbances in the plant, which is not practical. In servo drive systems, there are always some unknown

Manuscript was submitted for review on 23, August, 2017.

This work was supported in part by the Fujian Provincial Natural Science Foundation of China under Grant 2017J01747.

Guoyang Cheng, Wentao Yu, and Jin-gao Hu are with the College of Electrical Engineering and Automation, Fuzhou University, Fuzhou, China (e-mail: cheng@fzu.edu.cn, 99912431@qq.com, hu\_jingao@163.com).

Cheng and Hu are also with the Fujian provincial key lab of new energy, power generation and conversion, China

Digital Object Identifier 10.30941/CESTEMS.2018.00051

disturbances, such as load torque and nonlinear effects, which have to be properly compensated in control system design if a more precise servo performance is desired. To remove the steady-state error caused by unknown constant disturbances, Peng et al. [23], [24] enhanced the CNF technique with an integral action. However, the performance of integration-based control is not robust against the variation of target reference or disturbance, e.g., a minor change in the amplitude of disturbance or target reference may call for a re-tuning of the parameters in order to maintain a satisfactory performance. This is undesirable for practical applications. To reject unknown disturbance without resorting to integral control, Cheng et al. [28] incorporates a disturbance estimation-compensation mechanism based on extended state observer, into the CNF control framework for servo systems subject to actuator saturation and disturbances. It turns out that, this control scheme is more effective in accommodating the amplitude variations of disturbance or target reference, and fast and accurate set-point tracking can be achieved. The design in [28] was formulated in continuous-time domain. It is noted that, for real applications, a controller designed in continuous-time domain eventually has to be discretized (a methodology called “design by emulation”), and the sampling frequency usually should be 30 times higher than the closed-loop bandwidth, otherwise there may be a significant deviation in the actual control performance with digital implementation. For nonlinear controllers, the mapping between continuous and discrete-time domains is more complicated, and an even higher sampling frequency might be necessary to guarantee the equivalence. In view of the above limitation, it seems more convenient to design controllers directly in the discrete-time domain whenever possible. Indeed, this is the motivation for developing the discrete-time counterpart of the control scheme reported in [28].

The outline of the paper is as follows. Section II presents the design of robust composite nonlinear control scheme in discrete-time domain (hereinafter referred to as DRCNC), which includes an extended state observer for disturbance rejection. In Section III, the closed-loop stability of DRCNC control system is analyzed. Section IV presents the application of the proposed control scheme to the position regulation problem on a permanent magnet synchronous motor (PMSM). Experimental results will be provided. Finally, some concluding remarks can be found in Section V.

## II. DRCNC DESIGN

Introduced in this section is a discrete-time version of robust composite nonlinear control, which incorporates a combination of linear and nonlinear control actions, and a disturbance rejection mechanism based on extended state observer. The control scheme can achieve desirable transient and steady-state performance in set-point tracking and at the same time has better robustness against the amplitude variations of disturbance or reference.

The plants considered in this paper are motor drive servo systems, which can be modeled as linear systems subject to input saturation and unknown disturbance, characterized by

$$\begin{cases} \mathbf{x}(k+1) = \mathbf{A}\mathbf{x}(k) + \mathbf{B} \cdot \text{sat}(u(k)) + \mathbf{E}d(k), & \mathbf{x}(0) = \mathbf{x}_0 \\ \mathbf{y}(k) = \mathbf{C}_1\mathbf{x}(k) \\ h(k) = \mathbf{C}_2\mathbf{x}(k) \end{cases} \quad (1)$$

where  $\mathbf{x} \in \mathbb{R}^n$ ,  $u \in \mathbb{R}$ ,  $\mathbf{y} \in \mathbb{R}^p$ ,  $h \in \mathbb{R}$  and  $d \in \mathbb{R}$  are respectively the state vector, control input, measurement output, controlled output and disturbance input of the system.  $\mathbf{A}$ ,  $\mathbf{B}$ ,  $\mathbf{C}_1$ ,  $\mathbf{C}_2$  and  $\mathbf{E}$  are appropriate dimensional constant matrices. The function,  $\text{sat}: \mathbb{R} \rightarrow \mathbb{R}$ , represents the actuator saturation defined as

$$\text{sat}(u(k)) = \text{sign}(u(k)) \cdot \min\{u_{\max}, |u(k)|\} \quad (2)$$

with  $u_{\max}$  being the saturation level of the input. The following assumptions on the given system are made:

- ①  $(\mathbf{A}, \mathbf{B})$  is stabilizable,
- ②  $(\mathbf{A}, \mathbf{C}_1)$  is detectable,
- ③  $(\mathbf{A}, \mathbf{B}, \mathbf{C}_2)$  and  $(\mathbf{A}, \mathbf{E}, \mathbf{C}_1)$  have no invariant zero at  $z = 1$ ,
- ④  $d$  is an unknown bounded disturbance with a limited rate of change,
- ⑤  $h$  is also measurable, i.e.,  $h$  is part of the measurement output  $\mathbf{y}$ .

These assumptions are fairly standard for tracking control. The task here is to design a controller for the system with disturbance such that the resulting controlled output would track a set-point reference  $r$  fast, smoothly and as accurately as possible.

In the following, the design procedure of DRCNC will be outlined in four steps, to be specific, the design of a linear control law, the design of nonlinear feedback law, the design of an extended state observer to estimate the unmeasurable states and unknown disturbance, and lastly, the combination of linear control law, nonlinear feedback law and the observer to form the final controller.

**STEP 1:** For the moment, all the state variables and the disturbance  $d$  are assumed to be measurable (Note the assumption here is obviously not practical, and it will be dropped at STEP 3). A linear control law with a disturbance compensation term can be designed for the system (1):

$$u_l(k) = \mathbf{F} \cdot \mathbf{x}(k) + f_r \cdot r + f_d \cdot d(k) \quad (3)$$

where  $\mathbf{F}$  is chosen such that 1)  $\mathbf{A} + \mathbf{B}\mathbf{F}$  is an asymptotically stable matrix, and 2) the closed-loop transfer function  $\mathbf{C}_2(z\mathbf{I} - \mathbf{A} - \mathbf{B}\mathbf{F})^{-1}\mathbf{B}$  has a dominant pair of poles with a small damping ratio, which in turn would lead to a fast rise time in the closed-loop system response. Next,  $f_r$  is chosen as

$$f_r = [\mathbf{C}_2(\mathbf{I} - \mathbf{A} - \mathbf{B}\mathbf{F})^{-1}\mathbf{B}]^{-1} \quad (4)$$

and  $f_d$  is then computed as

$$f_d = -f_r [\mathbf{C}_2(\mathbf{I} - \mathbf{A} - \mathbf{B}\mathbf{F})^{-1}\mathbf{E}] \quad (5)$$

Note that  $f_r$  and  $f_d$  are well defined as  $(\mathbf{A}, \mathbf{B}, \mathbf{C}_2)$  is assumed to have no invariant zeros at  $z = 1$ .

**STEP 2:** Choose a positive definite symmetric matrix  $\mathbf{W} \in \mathbb{R}^{n \times n}$ ,

and solve the following Lyapunov equation:

$$\mathbf{P} = (\mathbf{A} + \mathbf{BF})^T \mathbf{P} (\mathbf{A} + \mathbf{BF}) + \mathbf{W}, \quad (6)$$

for  $\mathbf{P} > 0$ . Such a solution is always existent as  $\mathbf{A} + \mathbf{BF}$  is asymptotically stable. Next, define

$$\mathbf{x}_s(k) = \mathbf{G}_r r + \mathbf{G}_d d(k) \quad (7)$$

with

$$\begin{cases} \mathbf{G}_r := (\mathbf{I} - \mathbf{A} - \mathbf{BF})^{-1} \mathbf{B} f_r, \\ \mathbf{G}_d := (\mathbf{I} - \mathbf{A} - \mathbf{BF})^{-1} (\mathbf{B} f_d + \mathbf{E}) \end{cases}$$

It is easy to verify that  $\mathbf{C}_2 \mathbf{x}_s(k) = r$ . The nonlinear feedback portion of DRCNC is then given by

$$u_n(k) = \rho(e(k)) \mathbf{F}_n [\mathbf{x}(k) - \mathbf{x}_s(k)] \quad (8)$$

with

$$\mathbf{F}_n = \mathbf{B}^T \mathbf{P} (\mathbf{A} + \mathbf{BF}),$$

where  $\rho(e(k)) \leq 0$  with  $e(k) = h(k) - r$ , is a smooth and non-positive function of  $|e(k)|$ , to be used to gradually change the closed-loop damping ratio to improve the transient performance. The choices of the design parameters,  $\rho(e(k))$  and  $\mathbf{W}$ , will be discussed later.

**STEP 3:** An observer will be designed to estimate the unmeasurable state variables and unknown disturbance. Here it is assumed that the measurement output matrix  $\mathbf{C}_1 \in \mathbb{R}^{p \times n}$  is of full row rank, i.e., there is no redundancy in the measurements. Choose a matrix  $\mathbf{C}_0 \in \mathbb{R}^{(n-p) \times n}$ , such that the matrix

$$\mathbf{T} := \begin{bmatrix} \mathbf{C}_1 \\ \mathbf{C}_0 \end{bmatrix} \in \mathbb{R}^{n \times n} \text{ is invertible. Note that if } \mathbf{C}_1 = \begin{bmatrix} \mathbf{I}_p & \mathbf{0}_{p \times (n-p)} \end{bmatrix},$$

then the matrix  $\mathbf{T}$  is simply the  $n$ th-order identity matrix. Define

$$\text{an extended state vector } \bar{\mathbf{x}} := \begin{pmatrix} \mathbf{T}\mathbf{x} \\ d \end{pmatrix} \in \mathbb{R}^{n+1}, \text{ and note that the}$$

disturbance  $d$  is assumed to have a limited rate of change, i.e.,  $d(k+1) = d(k) + \tau(k)$ , where  $|\tau(k)| \leq \tau_v$ , an augmented model can be obtained as follows:

$$\begin{cases} \bar{\mathbf{x}}(k+1) = \bar{\mathbf{A}} \cdot \bar{\mathbf{x}}(k) + \bar{\mathbf{B}} \cdot \text{sat}(u(k)) + \mathbf{N} \cdot \tau(k), \\ \mathbf{y}(k) = \bar{\mathbf{C}} \cdot \bar{\mathbf{x}}(k) \end{cases} \quad (9)$$

where

$$\bar{\mathbf{A}} = \begin{bmatrix} \mathbf{T}\mathbf{A}\mathbf{T}^{-1} & \mathbf{T}\mathbf{E} \\ \mathbf{0}_{1 \times n} & 1 \end{bmatrix}, \quad \bar{\mathbf{B}} = \begin{bmatrix} \mathbf{T}\mathbf{B} \\ 0 \end{bmatrix}, \quad \mathbf{N} = \begin{bmatrix} \mathbf{0} \\ 1 \end{bmatrix}, \quad \bar{\mathbf{C}} = \begin{bmatrix} \mathbf{I}_p & \mathbf{0} \end{bmatrix}.$$

Based on the assumptions about the plant model, it is easy to check  $(\bar{\mathbf{A}}, \bar{\mathbf{C}})$  is detectable. Thus, an observer, of either full order or reduced order, can be designed to estimate the extended state variables. In real-time control, it is more feasible to implement controllers with a smaller dynamical order. Clearly, the first  $p$  elements of extended state vector  $\bar{\mathbf{x}}$ , denoted by  $\bar{\mathbf{x}}_1$ , is readily available from the measurement output  $\mathbf{y}$ . To estimate the remaining  $n-p+1$  elements, denoted by  $\bar{\mathbf{x}}_2$ , the matrices in the augmented model (9) need to be partitioned in accordance with the dimensions of  $\bar{\mathbf{x}}_1$  and  $\bar{\mathbf{x}}_2$ , as follows:

$$\bar{\mathbf{A}} = \begin{bmatrix} \mathbf{A}_{11} & \mathbf{A}_{12} \\ \mathbf{A}_{21} & \mathbf{A}_{22} \end{bmatrix}, \quad \bar{\mathbf{B}} = \begin{bmatrix} \mathbf{B}_1 \\ \mathbf{B}_2 \end{bmatrix}, \quad \mathbf{N} = \begin{bmatrix} \mathbf{0} \\ \mathbf{N}_1 \end{bmatrix}$$

Following the design procedure of reduced-order observer in [24], an observer gain matrix  $\mathbf{L} \in \mathbb{R}^{n-p+1}$  is chosen such that the eigenvalues of  $\mathbf{A}_{22} + \mathbf{L}\mathbf{A}_{12}$  are placed in appropriate locations inside the open unit circle around the origin. Then the reduced-order observer is derived as:

$$\begin{cases} \boldsymbol{\eta}(k+1) = \mathbf{A}_o \cdot \boldsymbol{\eta}(k) + \mathbf{B}_u \cdot \text{sat}(u(k)) + \mathbf{B}_y \cdot \mathbf{y}(k) \\ \hat{\bar{\mathbf{x}}}_2(k) = \boldsymbol{\eta}(k) - \mathbf{L} \cdot \mathbf{y}(k) \end{cases} \quad (10)$$

with

$$\begin{cases} \mathbf{A}_o = \mathbf{A}_{22} + \mathbf{L}\mathbf{A}_{12}, \\ \mathbf{B}_y = \mathbf{A}_{21} + \mathbf{L}\mathbf{A}_{11} - \mathbf{A}_o \mathbf{L}, \\ \mathbf{B}_u = \mathbf{B}_2 + \mathbf{L}\mathbf{B}_1 \end{cases}$$

where  $\boldsymbol{\eta}$  is the internal state vector of the observer, and  $\hat{\bar{\mathbf{x}}}_2$  is the estimation of  $\bar{\mathbf{x}}_2$ . The estimation of extended state vector  $\bar{\mathbf{x}}$  is given by

$$\hat{\bar{\mathbf{x}}}(k) = \begin{pmatrix} \mathbf{y}(k) \\ \hat{\bar{\mathbf{x}}}_2(k) \end{pmatrix} = \begin{pmatrix} \mathbf{y}(k) \\ \boldsymbol{\eta}(k) - \mathbf{L} \cdot \mathbf{y}(k) \end{pmatrix}$$

The estimations of the original state vector  $\mathbf{x}$  and unknown disturbance  $d$  can be obtained as:

$$\begin{pmatrix} \hat{\mathbf{x}}(k) \\ \hat{d}(k) \end{pmatrix} = \begin{bmatrix} \mathbf{T}^{-1} & \mathbf{0} \\ \mathbf{0} & 1 \end{bmatrix} \hat{\bar{\mathbf{x}}}(k) \quad (11)$$

**STEP 4:** In this step, the linear control law, the nonlinear feedback portion, and the reduced-order observer derived in the previous steps are combined to form the final controller. Note that the unmeasurable state variables and the unknown disturbance in the control law are now replaced with their estimated ones respectively. The DRCNC control law based on observer (10) is given by

$$\begin{cases} u(k) = \mathbf{F} \cdot \hat{\mathbf{x}}(k) + f_r \cdot r + \mu f_d \cdot \hat{d}(k) + \rho(e(k)) \mathbf{F}_n [\hat{\mathbf{x}}(k) - \hat{\mathbf{x}}_s(k)], \\ \hat{\mathbf{x}}_s(k) = \mathbf{G}_r \cdot r + \mathbf{G}_d \cdot \hat{d}(k) \end{cases} \quad (12)$$

where  $\mu \in [0, 1]$  is the discount factor for disturbance compensation. As the estimation  $\hat{d}(k)$  is influenced by noise and might include some uncertainty of plant model, using a value close to 1 for  $\mu$  is likely to result in over-compensation of disturbance, which could degrade the stability margins. Hence the parameter  $\mu$  should be tuned to trade off between the accuracy and robustness of controlled system.

The structure of DRCNC control scheme is illustrated in Fig. 1. The linear control law is the fundamental component of DRCNC, while the nonlinear feedback part is optional and can be used to speed up the transient process, and the extended state observer provides the estimations of state vector and disturbance if necessary. Such a modular structure offers a nice flexibility for control engineers.

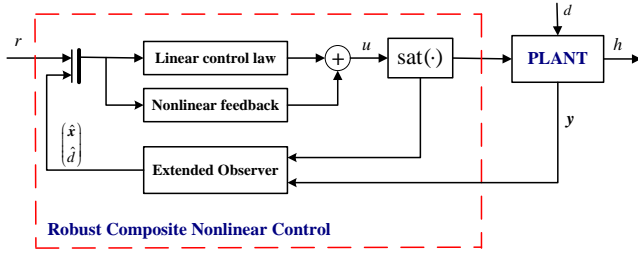


Fig. 1. Schematic diagram of the proposed control scheme.

### III. STABILITY ANALYSIS

To show that the control law (12) solves the set-point tracking control problem for the system (1), a matrix partition  $T^{-1} = [T_1 \quad T_2]$  is performed with  $T_1 \in \mathbb{R}^{n \times p}$ . Define

$$F_v = [FT_2 \quad \mu f_d], F_{nv} = [F_n T_2 \quad -F_n G_d], l_r = f_r + FG_r, \\ l_d = \mu f_d + FG_d.$$

Next, a positive definite matrix  $M \in \mathbb{R}^{(n-p+1) \times (n-p+1)}$  is chosen such that

$$M > F_v^T (B^T PB + F_n W^{-1} F_n^T) F_v \quad (13)$$

and then the following Lyapunov equation

$$Q = A_o^T Q A_o + M \quad (14)$$

is solved for a positive definite matrix  $Q$ . Note that such a  $Q$  exists as  $A_o$  is asymptotically stable.

**Theorem 1:** Consider the given system (1) with an unknown disturbance  $d$  whose magnitude and rate of change being bounded by non-negative scalars  $\tau_d$  and  $\tau_v$  respectively, i.e.,  $|d(k)| \leq \tau_d$ ,  $|\tau(k)| = |d(k+1) - d(k)| \leq \tau_v$ , there exists a scalar  $\hat{\rho} > 0$  such that for any  $\rho(e(k))$ , which is a smooth, non-positive function of  $e(k)$  with  $|\rho(e(k))| \leq \hat{\rho}$ , the observer-based DRCNC control law in (12) will ensure the closed-loop stability, meanwhile the system output  $h(k)$  will enter into a neighborhood of the step reference  $r$ , and the tracking error will asymptotically go to zero if  $\tau_v = 0$  (i.e., constant disturbance) and  $\mu = 1$ , provided that the following conditions are satisfied:

1) There exist two scalars  $\delta \in (0,1)$  and  $c_\delta > 0$  such that

$$\forall X \in \Omega(\delta, c_\delta) := \left\{ X \in \mathbb{R}^{2n-p+1} : X^T \begin{bmatrix} P & 0 \\ 0 & Q \end{bmatrix} X \leq c_\delta \right\} \\ \Rightarrow \left| [F \quad F_v] X \right| \leq (1-\delta)u_{\max} \quad (15)$$

2) The initial conditions,  $\mathbf{x}_0 = \mathbf{x}(0)$  and  $\boldsymbol{\eta}_0 = \boldsymbol{\eta}(0)$ , and  $d(0)$ , satisfy

$$\begin{pmatrix} \mathbf{x}_0 - \mathbf{x}_s(0) \\ \boldsymbol{\eta}_0 - L\mathbf{x}_{10} - \begin{pmatrix} \mathbf{x}_{20} \\ d(0) \end{pmatrix} \end{pmatrix} \in \Omega(\delta, c_\delta) \quad (16)$$

where  $\mathbf{x}_{10} \in \mathbb{R}^p$  and  $\mathbf{x}_{20} \in \mathbb{R}^{n-p}$  are the partitions of  $T\mathbf{x}_0$ , i.e.,

$$T\mathbf{x}_0 = \begin{pmatrix} \mathbf{x}_{10} \\ \mathbf{x}_{20} \end{pmatrix}.$$

3) The target reference  $r$  satisfies

$$|l_r \cdot r| \leq \delta u_{\max} - |l_d| \tau_d \quad (17)$$

**Proof.** Define

$$\boldsymbol{\xi}(k) = \hat{\mathbf{x}}_2(k) - \bar{\mathbf{x}}_2(k) = \boldsymbol{\eta}(k) - L\mathbf{y}(k) - \bar{\mathbf{x}}_2(k)$$

It is then easy to show that

$$\boldsymbol{\xi}(k+1) = A_o \cdot \boldsymbol{\xi}(k) - N_1 \cdot \tau(k) \quad (18)$$

Moreover, it can be verified that

$$\begin{pmatrix} \hat{\mathbf{x}}(k) - \mathbf{x}(k) \\ \hat{d}(k) - d(k) \end{pmatrix} = \begin{bmatrix} T_2 & \mathbf{0} \\ \mathbf{0} & 1 \end{bmatrix} \boldsymbol{\xi}(k) \quad (19)$$

Define  $\tilde{\mathbf{x}}(k) = \mathbf{x}(k) - \mathbf{x}_s(k)$ , then the control law in (12) can be rewritten as

$$u(k) = [F \quad F_v] \begin{pmatrix} \tilde{\mathbf{x}}(k) \\ \boldsymbol{\xi}(k) \end{pmatrix} + [l_r \quad l_d] \begin{pmatrix} r \\ d(k) \end{pmatrix} \\ + \rho(e(k)) [F_n \quad F_{nv}] \begin{pmatrix} \tilde{\mathbf{x}}(k) \\ \boldsymbol{\xi}(k) \end{pmatrix} \quad (20)$$

Next, the error dynamics of the plant in (1) can be expressed as,

$$\begin{aligned} \tilde{\mathbf{x}}(k+1) &= \mathbf{x}(k+1) - \mathbf{x}_s(k+1) \\ &= A\mathbf{x}(k) + B \cdot \text{sat}(u(k)) + Ed(k) - [x_s(k) + G_d \tau(k)] \\ &= A\tilde{\mathbf{x}}(k) + (A - I)x_s(k) + Ed(k) + B \cdot \text{sat}(u(k)) - G_d \tau(k) \\ &= A\tilde{\mathbf{x}}(k) + B \cdot [\text{sat}(u(k)) - l_r r - (f_d + FG_d)d(k)] - G_d \tau(k) \\ &= (A + BF)\tilde{\mathbf{x}}(k) + BF_v \boldsymbol{\xi}(k) + B\sigma(k) \\ &\quad - B(1-\mu)f_d d(k) - G_d \tau(k) \end{aligned} \quad (21)$$

where

$$\sigma(k) = \text{sat}(u(k)) - [F \quad F_v] \begin{pmatrix} \tilde{\mathbf{x}}(k) \\ \boldsymbol{\xi}(k) \end{pmatrix} - [l_r \quad l_d] \begin{pmatrix} r \\ d(k) \end{pmatrix} \quad (22)$$

For easy presentation, the time index ( $k$ ) will be omitted in the following derivation so long as no confusion is caused. Moreover, the variable  $e(k)$  of function  $\rho(e(k))$  will also be omitted hereinafter.

Now, for  $\begin{pmatrix} \tilde{\mathbf{x}} \\ \boldsymbol{\xi} \end{pmatrix} \in \Omega(\delta, c_\delta)$  and  $|l_r \cdot r| \leq \delta u_{\max} - |l_d| \tau_d$ , the

following condition holds:

$$\left| [F \quad F_v] \begin{pmatrix} \tilde{\mathbf{x}} \\ \boldsymbol{\xi} \end{pmatrix} + [l_r \quad l_d] \begin{pmatrix} r \\ d \end{pmatrix} \right| \\ \leq \left| [F \quad F_v] \begin{pmatrix} \tilde{\mathbf{x}} \\ \boldsymbol{\xi} \end{pmatrix} \right| + |l_r r| + |l_d| \tau_d \leq u_{\max} \quad (23)$$

Following the similar reasoning in [24], it can be shown that for the possible ranges of control signal  $u$  in (20), the term  $\sigma$  in (22) can be written as follows:

$$\begin{cases} \rho [F_n \quad F_{nv}] \begin{pmatrix} \tilde{\mathbf{x}} \\ \boldsymbol{\xi} \end{pmatrix} < \sigma \leq 0, & u < -u_{\max} \\ \sigma = \rho [F_n \quad F_{nv}] \begin{pmatrix} \tilde{\mathbf{x}} \\ \boldsymbol{\xi} \end{pmatrix}, & |u| \leq u_{\max} \\ 0 \leq \sigma < \rho [F_n \quad F_{nv}] \begin{pmatrix} \tilde{\mathbf{x}} \\ \boldsymbol{\xi} \end{pmatrix}, & u > u_{\max} \end{cases}$$

Thus  $\sigma$  can be rewritten in a unified form:

$$\sigma = \kappa\rho(\mathbf{F}_n\tilde{\mathbf{x}} + \mathbf{F}_{nv}\xi) \quad (24)$$

for some non-negative variable  $\kappa \in [0, 1]$ . Then the closed-loop system comprising the plant (1) and the observer-based control law (12) can be expressed as follows:

$$\mathbf{x}_\xi(k+1) = \mathbf{A}_\rho \cdot \mathbf{x}_\xi(k) - \mathbf{N}_d \cdot \bar{\mathbf{d}}(k) \quad (25)$$

where

$$\mathbf{x}_\xi = \begin{pmatrix} \tilde{\mathbf{x}} \\ \xi \end{pmatrix}, \quad \mathbf{A}_\rho = \begin{bmatrix} \mathbf{A} + \mathbf{B}\mathbf{F} + \kappa\rho\mathbf{B}\mathbf{F}_n & \mathbf{B}\mathbf{F}_\rho \\ \mathbf{0} & \mathbf{A}_o \end{bmatrix},$$

$$\mathbf{N}_d = \begin{bmatrix} \mathbf{B} & \mathbf{G}_d \\ \mathbf{0} & \mathbf{N}_1 \end{bmatrix}, \quad \bar{\mathbf{d}}(k) = \begin{pmatrix} (1-\mu)f_d d(k) \\ \tau(k) \end{pmatrix},$$

$$\mathbf{F}_\rho = \mathbf{F}_v + \kappa\rho\mathbf{F}_{nv}.$$

Define

$$\mathbf{P}_Q := \begin{bmatrix} \mathbf{P} & \mathbf{0} \\ \mathbf{0} & \mathbf{Q} \end{bmatrix},$$

and the Lyapunov function

$$V(k) = \mathbf{x}_\xi^T(k) \mathbf{P}_Q \mathbf{x}_\xi(k). \quad (26)$$

The increment of  $V(k)$  can be calculated along the trajectory of the closed-loop system (25):

$$\begin{aligned} \Delta V(k) &= V(k+1) - V(k) \\ &= -\tilde{\mathbf{x}}^T(k) \mathbf{W} \tilde{\mathbf{x}}(k) \\ &\quad + \tilde{\mathbf{x}}^T(k) \mathbf{F}_n^T (2\kappa\rho + \kappa^2 \rho^2 \mathbf{B}^T \mathbf{P} \mathbf{B}) \mathbf{F}_n \tilde{\mathbf{x}}(k) \\ &\quad + 2\tilde{\mathbf{x}}^T(k) \mathbf{F}_n^T (1 + \kappa\rho \mathbf{B}^T \mathbf{P} \mathbf{B}) \mathbf{F}_\rho \xi(k) \\ &\quad + \xi^T(k) \mathbf{F}_\rho^T \mathbf{B}^T \mathbf{P} \mathbf{B} \mathbf{F}_\rho \xi(k) - \xi^T(k) \mathbf{M} \xi(k) \\ &\quad - 2\bar{\mathbf{d}}^T(k) \mathbf{N}_d^T \mathbf{P}_Q \mathbf{A}_\rho \mathbf{x}_\xi(k) + \bar{\mathbf{d}}^T(k) \mathbf{N}_d^T \mathbf{P}_Q \mathbf{N}_d \bar{\mathbf{d}}(k) \end{aligned} \quad (27)$$

If  $\rho$  is chosen such that  $\rho \in [-2(\mathbf{B}^T \mathbf{P} \mathbf{B})^{-1}, 0]$ , then

$$2\kappa\rho + \kappa^2 \rho^2 \mathbf{B}^T \mathbf{P} \mathbf{B} \leq 0, \quad |1 + \kappa\rho \mathbf{B}^T \mathbf{P} \mathbf{B}| \leq 1$$

Hence,

$$\begin{aligned} \Delta V(k) &\leq -\tilde{\mathbf{x}}^T(k) \mathbf{W} \tilde{\mathbf{x}}(k) + 2(1 + \kappa\rho \mathbf{B}^T \mathbf{P} \mathbf{B}) \tilde{\mathbf{x}}^T(k) \mathbf{F}_n^T \mathbf{F}_\rho \xi(k) \\ &\quad + \xi^T(k) \mathbf{F}_\rho^T \mathbf{B}^T \mathbf{P} \mathbf{B} \mathbf{F}_\rho \xi(k) - \xi^T(k) \mathbf{M} \xi(k) \\ &\quad - 2\bar{\mathbf{d}}^T(k) \mathbf{N}_d^T \mathbf{P}_Q \mathbf{A}_\rho \mathbf{x}_\xi(k) + \bar{\mathbf{d}}^T(k) \mathbf{N}_d^T \mathbf{P}_Q \mathbf{N}_d \bar{\mathbf{d}}(k) \quad (28) \\ &= -\mathbf{x}_\xi^T(k) \mathbf{W}_\rho \mathbf{x}_\xi(k) - 2\bar{\mathbf{d}}^T(k) \mathbf{N}_d^T \mathbf{P}_Q \mathbf{A}_\rho \mathbf{x}_\xi(k) \\ &\quad + \bar{\mathbf{d}}^T(k) \mathbf{N}_d^T \mathbf{P}_Q \mathbf{N}_d \bar{\mathbf{d}}(k) \end{aligned}$$

where

$$\mathbf{W}_\rho := \begin{bmatrix} \mathbf{W} & -(1 + \kappa\rho \mathbf{B}^T \mathbf{P} \mathbf{B}) \mathbf{F}_n^T \mathbf{F}_\rho \\ * & \mathbf{M} - \mathbf{F}_\rho^T \mathbf{B}^T \mathbf{P} \mathbf{B} \mathbf{F}_\rho \end{bmatrix}$$

Note the element  $*$  can be inferred from symmetry of matrix. Since  $\mathbf{W} > 0$ , the matrix  $\mathbf{W}_\rho$  would be positive definite if the following condition is satisfied:

$$\mathbf{M} - \mathbf{F}_\rho^T \mathbf{B}^T \mathbf{P} \mathbf{B} \mathbf{F}_\rho - (1 + \kappa\rho \mathbf{B}^T \mathbf{P} \mathbf{B})^2 \mathbf{F}_n^T \mathbf{F}_n \mathbf{W}^{-1} \mathbf{F}_n^T \mathbf{F}_\rho > 0 \quad (29)$$

By the definition of  $\mathbf{M}$  in (13), there exists a scalar  $\hat{\rho} > 0$  such

that for any  $\rho(e(k))$ , which is a smooth and non-positive function of  $e(k)$  with  $|\rho(e(k))| \leq \hat{\rho}$ , the inequality (29) holds. For further derivation, a square positive matrix  $\mathbf{S}$  is introduced such that  $\mathbf{P}_Q = \mathbf{S}^T \mathbf{S}$ . Define

$$\lambda_m := \min \{ \lambda_{\min}(\mathbf{P}_Q^{-1} \mathbf{W}_\rho) : |\rho| \leq \hat{\rho} \},$$

$$\gamma_m := \max \{ \|\mathbf{S} \mathbf{P}_Q^{-1} \mathbf{A}_\rho^T \mathbf{P}_Q \mathbf{N}_d\| : |\rho| \leq \hat{\rho} \},$$

$$\lambda_n := \lambda_{\max}(\mathbf{N}_d^T \mathbf{P}_Q \mathbf{N}_d)$$

Note that  $\|\bar{\mathbf{d}}(k)\| \leq \sqrt{[(1-\mu)f_d \tau_d]^2 + \tau_v^2} := d_m$ . From (28), it can be obtained that

$$\begin{aligned} \Delta V(k) &\leq -\mathbf{x}_\xi^T(k) \mathbf{S}^T \mathbf{S} \mathbf{P}_Q^{-1} \mathbf{W}_\rho \mathbf{P}_Q^{-1} \mathbf{S}^T \mathbf{S} \mathbf{x}_\xi(k) \\ &\quad - 2\bar{\mathbf{d}}^T(k) \mathbf{N}_d^T \mathbf{P}_Q \mathbf{A}_\rho \mathbf{P}_Q^{-1} \mathbf{S}^T \mathbf{S} \mathbf{x}_\xi(k) \\ &\quad + \bar{\mathbf{d}}^T(k) \mathbf{N}_d^T \mathbf{P}_Q \mathbf{N}_d \bar{\mathbf{d}}(k) \\ &\leq -\lambda_{\min}(\mathbf{S} \mathbf{P}_Q^{-1} \mathbf{W}_\rho \mathbf{P}_Q^{-1} \mathbf{S}^T) \mathbf{x}_\xi^T(k) \mathbf{S}^T \mathbf{S} \mathbf{x}_\xi(k) \\ &\quad + 2\|\mathbf{S} \mathbf{P}_Q^{-1} \mathbf{A}_\rho^T \mathbf{P}_Q \mathbf{N}_d \bar{\mathbf{d}}(k)\| \cdot \|\mathbf{S} \mathbf{x}_\xi(k)\| \\ &\quad + \lambda_{\max}(\mathbf{N}_d^T \mathbf{P}_Q \mathbf{N}_d) \|\bar{\mathbf{d}}(k)\|^2 \\ &\leq -\lambda_{\min}(\mathbf{P}_Q^{-1} \mathbf{W}_\rho) \mathbf{x}_\xi^T(k) \mathbf{P}_Q \mathbf{x}_\xi(k) \\ &\quad + 2\gamma_m [\mathbf{x}_\xi^T(k) \mathbf{P}_Q \mathbf{x}_\xi(k)]^{1/2} \|\bar{\mathbf{d}}(k)\| + \lambda_n \|\bar{\mathbf{d}}(k)\|^2 \\ &\leq -\lambda_m \mathbf{x}_\xi^T(k) \mathbf{P}_Q \mathbf{x}_\xi(k) \\ &\quad + 2\gamma_m d_m [\mathbf{x}_\xi^T(k) \mathbf{P}_Q \mathbf{x}_\xi(k)]^{1/2} + \lambda_n d_m^2 \end{aligned} \quad (30)$$

Clearly, when  $[\mathbf{x}_\xi^T(k) \mathbf{P}_Q \mathbf{x}_\xi(k)]^{1/2} > \gamma$ , with

$$\gamma := \frac{d_m}{\lambda_m} \left( \gamma_m + \sqrt{\gamma_m^2 + \lambda_m \lambda_n} \right),$$

the closed-loop system with those assumptions, has  $\Delta V(k) < 0$ . Hence, the system is stable and its trajectory will converge into some place inside the space characterized by

$$\{ \mathbf{x}_\xi(k) \in \mathbb{R}^{2n-p+1} : \mathbf{x}_\xi^T(k) \mathbf{P}_Q \mathbf{x}_\xi(k) \leq \gamma^2 \}.$$

Noting that

$$\mathbf{x}_\xi^T(k) \mathbf{P}_Q \mathbf{x}_\xi(k) \geq \tilde{\mathbf{x}}^T(k) \mathbf{P} \tilde{\mathbf{x}}(k) \geq \lambda_{\min}(\mathbf{P}) \|\tilde{\mathbf{x}}(k)\|^2,$$

it is easy to obtain:

$$\|\tilde{\mathbf{x}}(k)\| \leq \frac{\gamma}{\sqrt{\lambda_{\min}(\mathbf{P})}}.$$

The tracking error,  $e(k) = h(k) - r = \mathbf{C}_2 \tilde{\mathbf{x}}(k)$ , is then bounded as

$$|e(k)| = |\mathbf{C}_2 \tilde{\mathbf{x}}(k)| \leq \|\mathbf{C}_2\| \|\tilde{\mathbf{x}}(k)\| \leq \frac{\gamma \|\mathbf{C}_2\|}{\sqrt{\lambda_{\min}(\mathbf{P})}} \quad (31)$$

Obviously, if  $\tau_v = 0$  (for constant disturbance) and  $\mu = 1$ , then  $\mathbf{x}_\xi(k) \rightarrow 0$  and  $e(k) \rightarrow 0$  as  $k \rightarrow \infty$ , i.e., the output  $h(k)$  asymptotically tracks the target reference  $r$  without any static bias.

This completes the proof of Theorem 1.

**Remark 1:** From the error dynamics in (25), it is clear that the

closed-loop poles can be changed by the nonlinear function  $\rho(e(k))$  and the gain matrix  $F_n$  which subsequently depends on the positive definite matrix  $W$ . The freedom in selecting  $W$  and  $\rho(e(k))$  is used to tune the control law so as to improve the transient performance as the controlled output  $h$  approaches the set point  $r$ . In general, one should try to choose  $W$  and  $\rho(e(k))$  such that the closed-loop poles at the steady state ( $e(k) \rightarrow 0$ ), have a dominant pair with a large damping ratio, which would yield a small overshoot. To simplify the selection process of  $W$ , one may consider limiting the choice of  $W$  to be a diagonal matrix and adjusting its diagonal weights through simulation.

**Remark 2:** The general guideline for selecting the nonlinear function  $\rho(e(k))$  is that it should be a smooth, non-positive function of  $e(k)$  such that  $\rho(e(k)) \in [-2(\mathbf{B}^T \mathbf{P} \mathbf{B})^{-1}, 0]$ . One possible choice of  $\rho(e(k))$  is given as follows:

$$\rho(e(k)) = -\frac{\beta}{1 + \alpha \alpha_0 \cdot |e(k)|} \quad (32)$$

where  $0 \leq \beta \leq 2(\mathbf{B}^T \mathbf{P} \mathbf{B})^{-1}$ . The positive parameter  $\alpha$  can modulate the speed of change in  $\rho(e(k))$ , while  $\alpha_0$  is used to normalize the initial tracking error:

$$\alpha_0 = \begin{cases} \frac{1}{|e(0)|}, & e(0) \neq 0, \\ 1, & e(0) = 0. \end{cases} \quad (33)$$

Obviously, the magnitude of  $\rho(e(k))$  starts from  $\beta/(1+\alpha)$  and increases to  $\beta$  as the system output  $h$  approaches the target reference  $r$ . Note that the choice of  $\rho(e(k))$  is non-unique.

#### IV. APPLICATION TO PMSM SERVO SYSTEM

In this section the proposed control scheme is applied to a permanent magnet synchronous motor (PMSM) position servo system. PMSM offers the advantages of compact structure, high power density and efficiency. So far, extensive applications of PMSM servo system have been reported (see e.g., [8], [9], [29-33]). PMSM servo systems typically adopt the vector control framework, so that the flux- and torque-producing components of the stator current are aligned along d (direct) and q (quadrature) axes respectively, thus enabling decoupled control of both the flux (d-axis) and torque (q-axis). In this work, a surface-mounted PMSM was taken as the plant, and its dq model can be given by

$$\begin{cases} \frac{d\theta_r}{dt} = \omega_r \\ T_e = 1.5n_p\psi i_q = J \frac{d\omega_r}{dt} + k_f \omega_r + T_L \\ u_q = R_s i_q + L_q \frac{di_q}{dt} + n_p \omega_r L_d i_d + n_p \omega_r \psi \\ u_d = R_s i_d + L_d \frac{di_d}{dt} - n_p \omega_r L_q i_q \end{cases} \quad (34)$$

where  $\theta_r$  and  $\omega_r$  are the mechanical angle and angular speed,

$T_e$  is the electromagnetic torque,  $T_L$  is the load torque,  $J$  is the motor inertia,  $k_f$  is the viscous friction coefficient,  $n_p$  is the number of pole pairs,  $\psi$  is the flux linkage established by permanent magnet,  $u_d$  and  $u_q$  are the voltage components for the d- and q-axes,  $i_d$  and  $i_q$  are the electric currents,  $L_d$  and  $L_q$  are the inductances,  $R_s$  is the stator resistance.

The field-oriented vector control scheme was adopted in the study, and the structure of the PMSM servo system is shown in Fig.2. The inner electric current loops are regulated by PI control laws, but the position and speed loops will be unified and controlled by one single controller. Taking the motor angular position  $\theta_r$  (rad) as the system output  $y$ , the angular position and velocity as the state variables, and  $i_q$  as the control signal  $u$  (to be used as the target reference for the  $i_q$  control loop), the following state-space model can be obtained:

$$\begin{cases} \dot{\mathbf{x}} = \mathbf{A}_p \cdot \mathbf{x} + \mathbf{B}_p \cdot (\text{sat}(u) + d) \\ y = \mathbf{C} \cdot \mathbf{x} \end{cases} \quad (35)$$

with

$$\mathbf{x} = \begin{pmatrix} \theta_r \\ \omega_r \end{pmatrix}, \mathbf{A}_p = \begin{bmatrix} 0 & 1 \\ 0 & 0 \end{bmatrix}, \mathbf{B}_p = \begin{bmatrix} 0 \\ b \end{bmatrix}, \mathbf{C} = [1 \quad 0]$$

where the parameter  $b = 1.5n_p\psi/J$ , and the lumped disturbance  $d = -(T_L + k_f\omega_r)/(1.5n_p\psi)$ . Note the viscous friction coefficient  $k_f$  usually has a small value. The PMSM in the study is of model 60CB020C (as shown in Fig. 3), with a rated torque of 0.64Nm, and the rated speed of rotation is 3000RPM. The number of pole pairs is 4. It has an optical encoder with a resolution of 2500 pulses for position measurement. The amplitude of the torque-producing current  $i_q$  is limited by 1.5A, i.e.,  $u_{\max} = 1.5$  A. The value of system parameter  $b$  in (35) has been identified as  $b=1920$ .

With a sampling period of  $T_s = 0.002$ s for digital implementation, the model (35) can be converted into the standard form (1) based on a zero-order hold discretization with the following parameter matrices:

$$\mathbf{A} = \begin{bmatrix} 1 & T_s \\ 0 & 1 \end{bmatrix}, \mathbf{B} = \mathbf{E} = \begin{bmatrix} \frac{1}{2}bT_s^2 \\ bT_s \end{bmatrix}, \mathbf{C}_1 = \mathbf{C}_2 = [1 \quad 0].$$

The DRCNC scheme, as outlined in Section II, was adopted to design the control law for position regulation here. First, a conjugate pair of closed-poles with the damping ratio  $\zeta = 0.3$  and natural frequency  $\omega = 30$  rad/s were chosen, and the linear feedback gain matrix was determined as

$$\mathbf{F} = -[0.4603 \quad 9.669 \times 10^{-3}]$$

The feed-forward gains were then computed as

$$f_r = 0.4603, f_d = -1$$

Next, a diagonal matrix  $\mathbf{W} = \text{diag}(0.001, 0.001)$  was chosen and

the nonlinear feedback gain matrix was computed as

$$F_n = [-0.0479 \quad 0.0534]$$

The nonlinear gain function was chosen as follows:

$$\rho(e(k)) = -0.8/(1+10\alpha_0 \cdot |e(k)|)$$

with  $\alpha_0$  determined as in (33), and  $e = y - r = \theta_r - r$ ,

where  $r = \theta_r^*$  (rad) is the target position for PMSM.

To estimate the unmeasurable speed and unknown disturbance, an observer of the form (10) was designed, of which the conjugate poles are organized in Butterworth pattern with the bandwidth  $\omega_0 = 100$  rad/s:

$$\begin{cases} \boldsymbol{\eta}(k+1) = \begin{bmatrix} 0.7363 & 3.334 \\ -9.043 \times 10^{-3} & 0.9826 \end{bmatrix} \cdot \boldsymbol{\eta}(k) \\ \quad + \begin{bmatrix} 3.334 \\ -0.0174 \end{bmatrix} \cdot \text{sat}(u(k)) + \begin{bmatrix} -19.70 \\ -1.271 \end{bmatrix} \cdot y(k), \\ \begin{pmatrix} \hat{\omega}_r(k) \\ \hat{d}(k) \end{pmatrix} = \boldsymbol{\eta}(k) + \begin{bmatrix} 131.9 \\ 4.522 \end{bmatrix} \cdot y(k) \end{cases}$$

Now, the DRCNC control law for position regulation can be written as follows:

$$\begin{aligned} u(k) = & \left\{ -\begin{bmatrix} 0.4603 & 9.669 \times 10^{-3} \end{bmatrix} + \rho(e(k)) \begin{bmatrix} -0.0479 & 0.0534 \end{bmatrix} \right\} \\ & \times \begin{pmatrix} e(k) \\ \hat{\omega}_r(k) \end{pmatrix} - 0.96 \hat{d}(k) \end{aligned} \quad (36)$$

For the two inner control loops of  $i_d$  and  $i_q$ , digital proportional-integral (PI) control laws were adopted. The PI parameters are:  $k_p = 46.2$ ,  $k_i = 0.185$ . The same values were applied to both loops. A sampling frequency of 20kHz was used for PI control implementation and space vector modulation

To make comparison, a linear controller with integration was also designed for position control, as follows:

$$\begin{cases} x_i(k+1) = x_i(k) + 0.1 \times [y(k) - r], \\ x_c(k+1) = 0.8187 \times x_c(k) + 3.492 \times \text{sat}(u(k)) + 16.43 y(k) \end{cases}$$

and

$$u(k) = \begin{bmatrix} -0.0607 & -0.5953 & -0.0250 \end{bmatrix} \cdot \begin{pmatrix} x_i(k) \\ y(k) - r \\ x_c(k) + 90.64 y(k) \end{pmatrix} \quad (37)$$

Note the linear controller (37) ensures that the closed-loop system has a pair of moderately-damped (0.707) poles to trade off the rise-time and overshoot. Moreover, it utilizes a reduced-order state observer with a bandwidth of 100 rad/s to estimate the motor speed.

To verify the design, control algorithms were implemented on a TMS320F28335 digital signal controller board from the Texas Instruments Corporation. Real-time experiments were subsequently carried out using the Code Composer Studio software system, and the collected data were then processed in MATLAB. Experiments were first conducted for target angle  $\pi$  under three different load torques (specifically, 0%, 50%, and 100% of the rated load, note that there is also some other

disturbance in the system), and the results are shown in Figs. 4 to 6. In the figures, the waveforms of motor position (rad), speed (rad/s), control signal (the command current  $i_q$ , A) and the actual  $i_q$  are presented. Comparisons are made between the DRCNC controller and the linear controller. It is obvious the servo system with DRCNC achieves superior performance in all the tracking tasks, and the settling times with a 2% error bound are 0.102s, 0.106s and 0.122s respectively, implying the impact of load disturbance is rejected effectively. Whereas the linear controller, which was carefully designed to produce a desirable performance (similar to that of DRCNC, as shown in Fig. 4) for target angle  $\pi$  with a 50% rated load, suffers a significant degradation when the load torque or the target angle is varied. To be specific, the system output with the linear controller experiences a noticeable overshoot (more than 20%) when the load is reduced to zero (see Fig.5) and has a sluggish response in the case of full load (see Fig.6). Moreover, when the target angle is stepped up to  $2\pi$  (see Fig.7), an overshoot (about 20%) appears on the system output (with linear control) again. In these cases, it may take a long time for the system output to settle down to the target position. This implies that it would be difficult to design a linear controller (with integration) which could achieve satisfactory performance for various working conditions.

Fig. 8 gives the results of DRCNC for target angle  $2\pi$  under null and full loads respectively. It is clear the output response slows down with a large load torque. As the control signal (command current) gets saturated for target  $2\pi$  at the beginning, the load torque cannot be fully compensated at the transient process, but its impact eventually will be removed at the steady state. On the whole, the output performances for  $2\pi$  with DRCNC are still desirable for various load conditions. Finally, to study the performance with respect to the variation of system parameter  $b$ , the value of  $b$  in the DRCNC controller was perturbed by  $\pm 25\%$  respectively (the values of other design parameters remained unchanged) for experimental test, and the results are shown in Fig. 9. Some degradations can be observed in the transient process (an increased overshoot for the parameter  $b$  below its nominal value, and a slower response for a larger  $b$  value), but the system output can settle accurately onto the target position. The overall performance is acceptable for the given range of variation. The proposed control scheme has some degree of performance robustness against the model uncertainty. For future research, it would be interesting to conduct a theoretical analysis of the robustness issue related with the perturbation in parameter  $b$ .

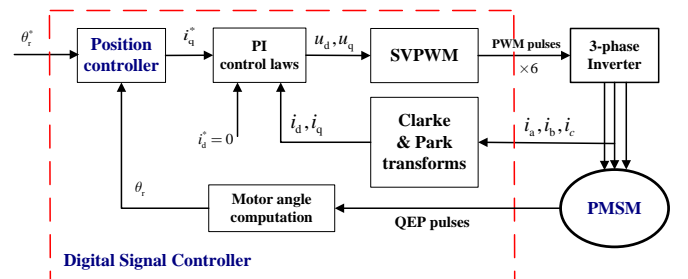


Fig. 2. Schematic diagram of PMSM position servo system.



Fig. 3. Experimental setup of PMSM servo system.

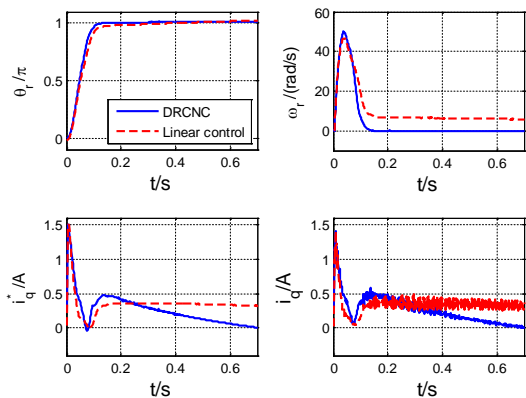


Fig. 4. Comparison of experimental results for target angle  $\pi$  under a 50% rated load.

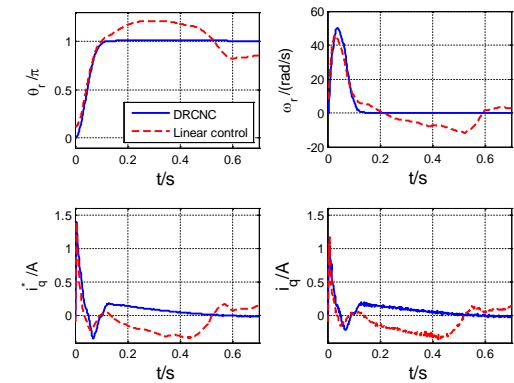


Fig. 5. Comparison of experimental results for target angle  $\pi$  without load.

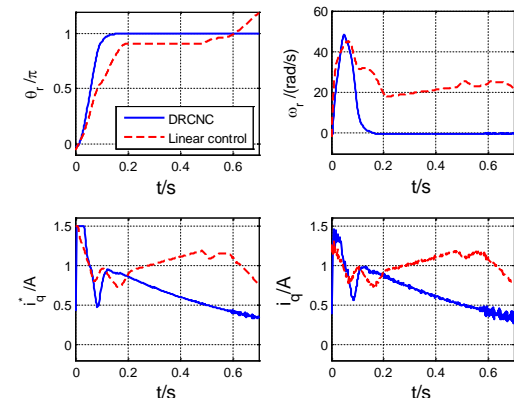


Fig. 6. Comparison of experimental results for target angle  $\pi$  under a 100% rated load.

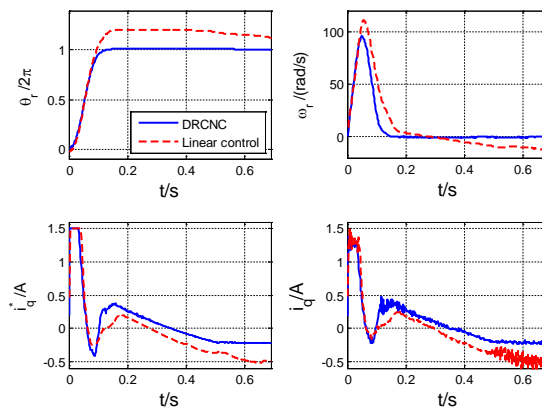


Fig. 7. Comparison of experimental results for target angle  $2\pi$  under a 50% rated load.

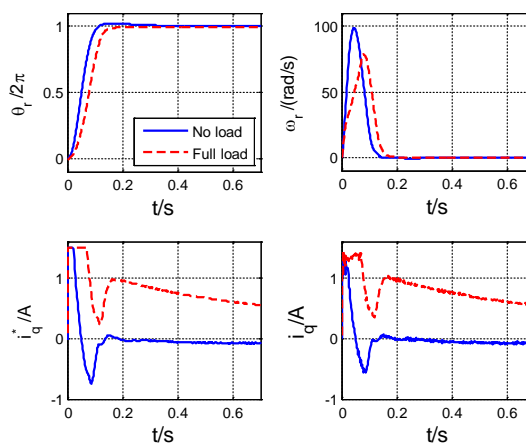


Fig. 8. Experimental results of DRCNC for target angle  $2\pi$  under null and full rated load.

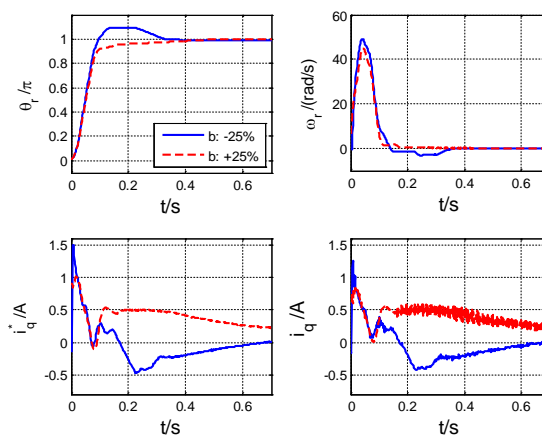


Fig. 9. Experimental results of DRCNC with parameter variations for target angle  $\pi$  and a 50% rated load.

### V. CONCLUSION

This paper has presented a new control scheme, which combines a linear control law, a nonlinear feedback part, and an ESO-based disturbance rejection mechanism together, so as to achieve superior transient and steady-state set-point tracking performance for motor servo systems with actuator saturation and disturbances. This control scheme has been utilized to

design a PMSM position servo system. Experimental results show that the design is capable of achieving faster settling with robustness. The proposed control scheme has a great potential for performance improvement in many industrial servo systems.

## REFERENCES

- [1] Y.Li, K.H. Ang, and G. Chong, "Patents, software, and hardware for PID control – an overview and analysis of the current art," *IEEE Control Systems Magazine*, vol.26, no.2, pp.42-54, Apr.2006.
- [2] K. Li, "PID tuning for optimal closed-loop performance with specified gain and phase margins," *IEEE Trans. Control Syst. Technol.*, vol.21, no.3, pp.1024-1030, May 2013.
- [3] Y.X. Su, D.Sun, and B.Y.Duan, "Design of an enhanced nonlinear PID controller," *Mechatronics*, vol.15, no.9, pp.1005-1024, Dec.2005.
- [4] M.F. Heertjes, X.G.P. Schuurbijs, and H. Nijmeijer, "Performance improved design of N-PID controlled motion systems with applications to wafer stages," *IEEE Trans. Ind. Electron.*, vol.56, no.5, pp.1347-1355, May 2009.
- [5] J.W. Choi, and S.C.Lee, "Antiwindup strategy for PI-type speed controller," *IEEE Trans. Ind. Electron.*, vol.56, no.6, pp.2039-2046, Jun.2009.
- [6] H.B. Shin, and J.G.Park, "Anti-windup PID controller with integral state predictor for variable-speed motor drives," *IEEE Trans. Ind. Electron.*, vol.59, no.3, pp.1509-1516, Mar.2012.
- [7] B. Hunnekens, N van deWouw, M. Heertjes, and et al. "Synthesis of variable gain integral controllers for linear motion systems," *IEEE Trans. Control Syst. Technol.*, vol.23, no.1, pp.139-149, Jan.2015.
- [8] X. Guan, and Y.Li, "Variable gain PI control method for permanent magnet synchronous motor based on load torque feedback real-time compensation," *Transactions of China Electrotechnical Society*, vol.31, no.23, pp.38-45, Dec. 2016(in Chinese).
- [9] H. Fu, Y.F.Zuo, C. Liu, and J.Zhang, "A variable input gain proportional integral controller for permanent magnetic synchronous motor speed regulation system," *Transactions of China Electrotechnical Society*, vol.32, no.1, pp.168-174, Jan.2017(in Chinese).
- [10] J.Q.Han, "Active disturbance rejection controller and its application," *Control and Decision*, vol.13, no.1, pp.19-23, Jan.1998(in Chinese).
- [11] J.Q.Han, "From PID to active disturbance rejection control," *IEEE Trans. Ind. Electron.*, vol.56, no.3, pp.900-906, Mar.2009.
- [12] Q.Zheng, L.Dong, DH Lee, and et al. "Active disturbance rejection control for MEMS gyroscopes," *IEEE Trans. Control Syst. Technol.*, vol.17, no.6, pp.1432-1438, Nov.2009.
- [13] D. Wu, T. Zhao, and K.Chen, "Research and industrial applications of active disturbance rejection control to fast tool servos," *Control Theory & Applications*, vol.30, no.12, pp.1354-1362, Dec. 2013(in Chinese).
- [14] H. Tang, and Y.Li, "Development and active disturbance rejection control of a compliant micro/nano-positioning piezo-stage with dual mode," *IEEE Trans. Ind. Electron.*, vol.61, no.3, pp.1475-1492, Mar.2014.
- [15] B. Guo, Z. Wu, and H.Zhou, "Active disturbance rejection control approach to output-feedback stabilization of a class of uncertain nonlinear systems subject to stochastic disturbance," *IEEE Trans. Autom. Control*, vol.61, no.6, pp.1613-1618, Jun.2016.
- [16] Y.F.Zuo, J.Zhang, C.Liu, and T.Zhang, "Integrated design for permanent magnet synchronous motor servo systems based on active disturbance rejection control," *Transactions of China Electrotechnical Society*, vol.31, no.11, pp.51-58, Nov.2016.(in Chinese).
- [17] D.Yoo, S.T. Yau, Z. Gao, "Optimal fast tracking observer bandwidth of the linear extended state observer," *International Journal of Control*, vol.80, no.1, pp.102-111, Jan.2007.
- [18] Z.Q. Chen, M.W. Sun, and R.G.Yang, "On the stability of linear disturbance rejection control," *Acta Automatica Sinica*, vol.39, no.5, pp.574-580, May 2013. (in Chinese).
- [19] W. Tan, and C. Fu, "Linear active disturbance rejection control: analysis and tuning via IMC," *IEEE Trans. Ind. Electron.*, vol.63, no.4, pp.2350-2359, Apr.2016.
- [20] G. Herbst, "Practical active disturbance rejection control: bumpless transfer, rate limitation and incremental algorithm," *IEEE Trans. Ind. Electron.*, vol.63, no.3, pp.1754-1762, Mar.2016.
- [21] Z. Lin, M. Pachter and S. Banda, "Toward improvement of tracking performance – Nonlinear feedback for linear system," *International Journal of Control*, vol. 70, no.1, pp.1-11, Jan.1998.
- [22] B. M. Chen, T. H. Lee, K. Peng and V. Venkataramanan, "Composite nonlinear feedback control for linear systems with input saturation: Theory and an application," *IEEE Trans. Autom. Control*, vol. 48, pp. 427-439, Mar.2003.
- [23] K. Peng, B. M. Chen, G. Cheng and T. H. Lee, "Modeling and compensation of nonlinearities and friction in a micro hard disk drive servo system with nonlinear feedback control," *IEEE Trans. Control Syst. Technol.*, vol.13, no.5, pp.708-721, Sep.2005.
- [24] K. Peng, G. Cheng, B. M. Chen, and T. H. Lee, "Improvement of transient performance in tracking control for discrete-time systems with input saturation and disturbances," *IET Control Theory Appl.*, vol. 1, no. 1, pp. 65-74, Jan. 2007.
- [25] K. Peng, G. Cai, B. M. Chen, and et al. "Design and implementation of an autonomous flight control law for a UAV helicopter," *Automatica*, vol.45, no.10, pp.2333-2338, Oct. 2009.
- [26] G. Cai, B. M. Chen, X. Dong, and T. H. Lee, "Design and implementation of a robust and nonlinear flight control system for an unmanned helicopter," *Mechatronics*, vol.21, no.5, pp.803-820, Aug. 2011.
- [27] S. Eren, M. Pahlevaninezhad, A.Bakshshai, and et al. "Composite nonlinear feedback control and stability analysis of a grid-connected voltage source inverter with LCL filter," *IEEE Trans. Ind. Electron.*, vol.60, no.11, pp.5059-5074, Nov.2013.
- [28] G. Cheng, K. Peng, "Robust composite nonlinear feedback control with application to a servo positioning system," *IEEE Trans. Ind. Electron.*, vol.54, no.2, pp.1132-1140, Apr.2007.
- [29] H. Lee and J. Lee, "Design of iterative sliding mode observer for sensorless PMSM control," *IEEE Trans. Control Syst. Technol.*, vol.21, no.4, pp. 1394-1399, Jul. 2013.
- [30] G. Prior and M. Krstic, "Quantized-input control Lyapunov approach for permanent magnet synchronous motor drives," *IEEE Trans. Control Syst. Technol.*, vol.21, no.5, pp. 1784-1794, Sep.2013
- [31] W. Yu, Y. Luo, and Y. Pi, "Fractional order modeling and control for permanent magnet synchronous motor velocity servo system," *Mechatronics*, vol.23, no.7, pp.813-820, Oct. 2013.
- [32] G. Cheng, J. Hu, "An observer-based mode switching control scheme for improved position regulation in servomotors," *IEEE Trans. Control Syst. Technol.*, 2014, 22(5):1883-1891.
- [33] J. Shen, X. Qin, and Y. Wang, "High-speed permanent magnet electrical machines - applications, key issues and challenges," *CES Transactions on Electrical Machines and Systems*, vol. 2, no. 1, pp.23-33, Mar. 2018.



**Guoyang Cheng** (M'06–SM'14) received the B.Eng. degree in information systems from the National University of Defense Technology, Changsha, China, in 1992, the M.Eng. degree in control engineering from Tsinghua University, Beijing, China, in 1995, and the Ph.D. degree from the National University of Singapore (NUS), Singapore, in 2006. From 1995 to 2001, he was a Computer Engineer in Xiamen, China. From 2005 to 2006, he was a Research Engineer with the Department of Electrical and Computer Engineering, NUS. Since 2006, he has been with the College of Electrical Engineering and Automation, Fuzhou University, Fuzhou, China, where he is now a professor. His research interests include power drive, motion control and mechatronics systems. He is an IEEE Senior Member, and currently serves as an associate editor for the IET journal *Electronics Letters*.



**Wentao Yu** received the bachelor's degree from the Wuhan University of Technology, Wuhan, China, in 2007 and the master's degree from the East China University of Technology, Nanchang, China, in 2013. He is currently pursuing the Ph.D. degree at the College of Electrical Engineering and Automation, Fuzhou University, Fuzhou, China. He has been engaged in the research of motor drive technology for 12 years, and now his research interests are in the area of AC servo system, with emphasis on parameter identification and robust nonlinear control of motor drive system.



**Jin-gao Hu** was born in Fujian, China, in 1962. He received the bachelor's degree in industrial automation from Donghua University, Shanghai, China, in 1983, and the M.Eng. degree from the same university in 1986. Since 1986, he has been with the College of Electrical Engineering and Automation, Fuzhou University, Fuzhou, China. He has been engaged in R&D activities, covering the broad area of motor motion control, power electronics, embedded computer system and their applications, with more than 30 years' experience.